



HAL
open science

Cirrus Climatological Results from Lidar Measurements at OHP (44 °N, 6 °E)

Leah Goldfarb, Philippe Keckhut, Marie-Lise Chanin, Alain Hauchecorne

► **To cite this version:**

Leah Goldfarb, Philippe Keckhut, Marie-Lise Chanin, Alain Hauchecorne. Cirrus Climatological Results from Lidar Measurements at OHP (44 °N, 6 °E). *Geophysical Research Letters*, 2001, 28 (9), pp.1687-1690. 10.1029/2000GL012701 . hal-01633087

HAL Id: hal-01633087

<https://hal.science/hal-01633087>

Submitted on 11 Nov 2017

HAL is a multi-disciplinary open access archive for the deposit and dissemination of scientific research documents, whether they are published or not. The documents may come from teaching and research institutions in France or abroad, or from public or private research centers.

L'archive ouverte pluridisciplinaire **HAL**, est destinée au dépôt et à la diffusion de documents scientifiques de niveau recherche, publiés ou non, émanant des établissements d'enseignement et de recherche français ou étrangers, des laboratoires publics ou privés.

Cirrus Climatological Results from Lidar Measurements at OHP (44 ° N, 6 ° E)

L. Goldfarb, P. Keckhut, M.-L. Chanin, and A. Hauchecorne

CNRS/Service d'Aéronomie, Verrières-le-Buisson, France

Abstract. A climatology of cirrus clouds over the Observatoire de Haute Provence in France has been constructed from the analysis of ground-based lidar measurements taken from 1997 to 1999. During this period the high-resolution Rayleigh/Mie lidar collected 384 nights of measurements and cirrus profiles are observed in about half of these cases. We find subvisible cirrus ($\tau < 0.03$) constitute $\sim 20\%$ of cirrus cloud occurrences and that the mean thickness of a subvisible cirrus cloud layer is less than 1 km. A discussion of the error associated with these determinations is also presented.

Introduction

Cirrus clouds cover about 30 % of the earth's surface. They impact the radiation budget [Liou, 1986], which in turn governs the global climate. Cirrus clouds have also been invoked as a possible surface for heterogeneous reactions that could impact ozone concentrations in the upper troposphere and lower stratosphere (UT/LS) [Borrmann *et al.*, 1996]. Characterizing cirrus occurrences and their optical properties is critical for climate models, but there are very few data. (See Penner *et al.* [1999] for an overview.)

In particular characterizing optically thin cirrus has been acknowledged [Rosenfield *et al.*, 1998] as an important, albeit difficult, task for calculating heating rates. Cirrus clouds with optical thicknesses (τ) less than 0.03 are known as subvisible cirrus (SVC) [Sassen *et al.*, 1989]. Most attention has been focused in the tropics where the highest occurrence frequency ($\sim 20\%$) of SVC have been observed by SAGE (Stratospheric Aerosol and Gas Experiment) II [Wang *et al.*, 1996, 1998]. This satellite instrument is very sensitive to optically thin cirrus ($\tau_{\text{threshold}} \sim 2 \times 10^{-4}$). The prevalence of these clouds in the tropics is important, because the radiative effects of SVC are expected to be the greatest ($+ 0.5 \text{ W m}^{-2}$) [Wang *et al.*, 1996] in this region. However, global cirrus statistics are needed for accurate climate simulations. Ground-based measurements are an excellent way to obtain high-resolution cirrus data to complement satellite data.

The objective of this study is to construct a cirrus climatology using lidar measurements from the Observatoire de Haute Provence (OHP), France. Our measurements have a high altitude resolution (75 m) and confirm the presence of SVC at northern midlatitudes. SVC have been observed by others using ground-based instrumentation at midlatitudes (e.g., Reichardt [1999]). Indeed, the SVC optical thickness threshold was determined using midlatitude (45 ° N, 90 ° W)

lidar data [Sassen *et al.*, 1989]. Most ground-based studies of SVC have been limited in scope (e.g. see Sassen and Cho [1992]) and thus extracting climatological data from lidar work has been quite challenging. Our findings are distinctive because they are based on the most exhaustive record of ground-based cirrus observations.

Instrumentation

The Rayleigh/Mie lidar at OHP makes measurements during the night throughout the year. OHP is situated at 43.9 ° N, 5.7 ° E and at 679 m altitude. We give an overview of the instrumentation here; details can be found elsewhere [Keckhut *et al.*, 1993; Hauchecorne *et al.*, 1992]. A doubled Nd-YAG laser which emits a light pulse of ~ 10 ns at 532.2 nm is operated at a repetition rate 50 Hz with an average pulse energy of 300 mJ. This zenith pointing lidar functions in cirrus mode between 100 - 150 nights per year.

The OHP lidar has an extensive altitude range (1 - 80 km), but the description of the detection system given here is limited to that which has been optimized for the UT/LS. The receiving telescope has an adjustable diaphragm that allows a maximum diameter of 20 cm. The altitude range for this telescope is between 1 and 25 km. The photon counting system has a 0.5 ms bin width corresponding to an altitude resolution of 75 m; the received backscatter signal is averaged over 160 seconds intervals. The lidar is operated in semi-automatic mode (i.e., signal collection is stopped only if precipitation occurs or with the onset of dawn). A typical measurement period is 6 hours. Presently the OHP lidar is not equipped with a polarizing detector, thus no information about the size or phase of the aerosols is obtained. Atmospheric temperature measurements are taken from high-resolution (Vaisala RS80) radiosondes launched from Nimes (~ 120 km east of OHP).

Analysis

A scattering ratio (SR) is calculated from the sum of the Mie (aerosol) and Rayleigh scattering coefficients, ($\beta_{\text{aerosol}} + \beta_{\text{Rayleigh}}$, respectively), divided by the Rayleigh backscatter coefficient:

$$SR = \frac{\beta_{\text{aerosol}} + \beta_{\text{Rayleigh}}}{\beta_{\text{Rayleigh}}}$$

The numerator corresponds to the raw lidar signal, corrected for the background and the altitude squared dependence. The denominator is obtained using a fourth degree polynomial fit to the backscattered profile after the removal of the Mie component. When no aerosols are present, the SR equals one. Typically, for clear-sky conditions, the SR standard deviation at low altitudes (5 - 6 km) is ~ 0.04 and increases to ~ 0.4 at high altitudes (18 - 19 km). This rise in the standard deviation is due to the exponential decay in

Copyright 2001 by the American Geophysical Union.

Paper number 2000GL012701.
0094-8276/01/2000GL012701\$05.00

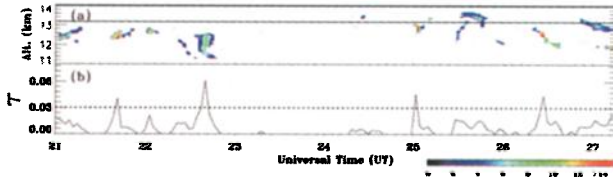


Figure 1. Analyzed lidar data for the night of July 11 - 12, 1998. The scattering ratio is shown in Panel (a); the scale is in the lower right. Only scattering ratios greater than t_{SR} (see text) are shown in the color plot. The solid line is the height of the tropopause. Panel (b) displays the optical thickness, τ ; the dotted line is the SVC threshold. For this particular observation, no clouds/aerosols are observed below 11 km.

the signal with altitude. The minimum detectable optical depth for the OHP lidar is 1×10^{-3} .

The presence of cirrus is determined when the following two criteria are met: the SR is greater than the defined threshold (t_{SR}) and the cloud layer is situated in an air mass with a temperature of -25°C or colder. The t_{SR} is defined as the sum of the nightly mean SR from 18 - 19 km plus three times the SR standard deviation for this altitude range (d_{SR}). Because the t_{SR} is defined for each nightly determination (cloudy or clear sky), it is sensitive to the signal to noise of the particular observation. The d_{SR} is slightly greater when thick clouds are present, thus there is a slight bias against seeing thin clouds under these conditions. The -25°C threshold, as determined from the radiosondes, has been recognized (Heymsfield, private communication) as an indicator of cirrus. Cirrus occurrence frequencies are calculated from the number of cirrus occurrences divided by the total number of measurements.

The optical thickness of a cirrus cloud is calculated from the integral of the extinction coefficient, $\alpha(z)$:

$$\tau_{\text{cirrus}} = \int_{z_{\min}}^{z_{\max}} \alpha(z) dz,$$

where z_{\min} and z_{\max} represent the minimum and maximum cirrus altitude, respectively. Using the SR and the lidar ratio, $LR = (\alpha/\beta_{\text{aerosol}})$, we can derive the relationship used to calculate the optical thickness of cirrus:

$$\tau_{\text{cirrus}} = (LR) \sigma_{\text{Rayleigh}} \int_{z_{\min}}^{z_{\max}} n_{\text{air}}(z) (SR(z) - 1) dz,$$

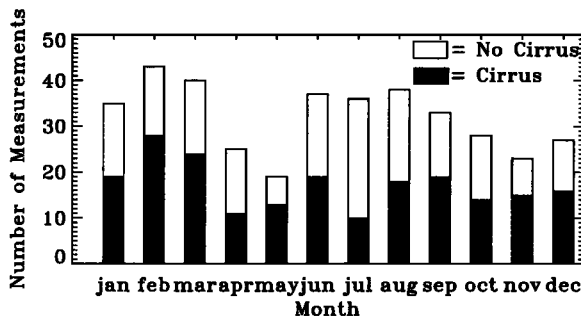


Figure 2. A histogram of the number of cirrus occurrences and the total number of nightly measurements from 1997 - 1999 as a function of month.

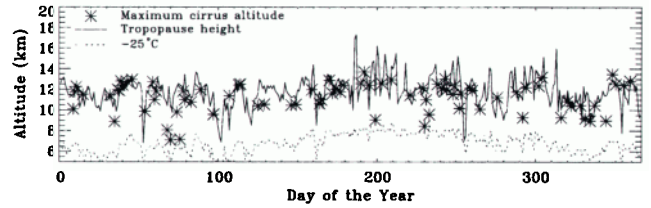


Figure 3. A profile of cirrus cloud top heights for 1998. Stars denote the maximum cirrus altitude, the solid line is the tropopause height and the dotted line marks altitudes that corresponds to -25°C . The tropopause and -25°C altitudes are determined from radiosondes measurements.

where, σ_{Rayleigh} = Rayleigh backscattering cross section, $\beta_{\text{Rayleigh}} = \sigma_{\text{Rayleigh}} n_{\text{air}}(z)$, and $n_{\text{air}}(z)$ = density of air, as calculated by the MSIS-E-90 atmosphere model [<http://nssdc.gsfc.nasa.gov/space/model/models/msis.html>]. A LR of 18.2 sr [Platt and Dille, 1984] is used, and $\sigma_{\text{Rayleigh}}(532\text{ nm}) = 5.7 \times 10^{-32} \text{ m}^2 \text{ sr}^{-1}$. No corrections for multiple scattering are made.

Results

From 1997 to 1999 the lidar system took 384 nights of measurements. The capacity of the OHP lidar to accurately measure optical thicknesses of SVC is illustrated in Figure 1. As seen in Figure 2, cirrus clouds are observed in half of the cases (54 %). The cirrus occurrence frequencies for spring, summer, winter, and fall are 57 %, 42 %, 57 %, 60%, respectively.

Figure 3 shows the location of the cloud top heights for 1998 in relation to the tropopause; altitudes that correspond to -25°C are also presented in the plot. We use the WMO's definition of the tropopause (the altitude where the temperature lapse rate decreases to 2 K km^{-1} for at least 2 km). All temperatures are obtained from the radiosondes. Figure 3 indicates that even with the daily variability of the tropopause height, the cirrus cloud tops tend to consistently track the tropopause. Results for 1997 and 1999 are similar. A histogram of the location of the cloud top heights with respect to the tropopause is presented in Figure 4. A significant portion, 53 %, of the cirrus cloud top heights are within 0.75 km of the tropopause.

Table 1 summarizes the statistics for cirrus frequencies for individual layers and their total thickness for the three years studied. A separation of 3 channels (corresponding to 225 m) is needed for a new layer to be declared. The mean cirrus thickness is $1.4 \pm 1.3 \text{ km}$ and centered at $10.0 \pm 1.3 \text{ km}$, while the SVC are markedly thinner ($0.8 \pm 0.7 \text{ km}$) but are located in the same region ($10.4 \pm 1.5 \text{ km}$).

We present the seasonality of the optical thicknesses in Figure 5; the results are binned on a log scale to better perceive the cases of very optically thin clouds. The SVC occurrence percentages for spring, summer, fall, and winter are 23 %, 18 %, 21 %, 25 %, respectively. When the mean for all three years is taken, cirrus with optical depths between 0.03 and 0.1 are the most prevalent. This pattern is similar for the annual results, except for 1998 where cirrus with optical thickness between 0.01 and 0.03 are as frequent as those between 0.03 and 0.1. The SVC cloud occurrence varies from year to year, 22 % (1997), 27 % (1998), 17 % (1999).

Table 1. Cirrus cloud statistics for multilayer occurrences and mean cirrus cloud thickness. Values in parenthesis are for SVC only.

	1997		1998		1999		1997 - 1999	
	% Cloud Occurrence							
1 layer	36	(13)	38	(20)	30	(8)	36	(14)
2 layers	14	(7)	14	(5)	21	(9)	16	(7)
3 layers	4	(2)	2	(2)	1	(0)	2	(2)
	km							
Mean layer thickness	1.5	(0.8)	1.3	(0.8)	1.5	(0.7)	1.4	(0.8)
Stdev	1.3	(0.6)	1.1	(0.6)	1.4	(0.8)	1.3	(0.7)
No. of cirrus occurrences	75	(30)	80	(39)	51	(17)	206	(86)

Discussion

The OHP data set offers a unique perspective on cirrus clouds at northern midlatitudes. Unlike campaign data or satellite observations, the lidar measurements presented here were systematically taken over the period of three years, with excellent altitudinal and temporal resolution. Analysis has revealed many optically thin and SVC events, with the latter composing 23 % of the occurrences. Profiles such as those shown in Figure 1 show that cirrus events can be highly variable both temporally and spatially. Annual variation for some of the cirrus statistics (e.g., the mean cirrus thickness) is observed.

Certain considerations must be taken into account when analyzing the OHP lidar data. With the ground-based lidar technique it is not possible to make measurements when there are opaque/precipitating clouds. Consequently it is possible that our statistics may be biased, especially the number of cirrus occurrences in the optical depth range of 0.3 - 1.0, category F in Figure 5. Generally at OHP there are only ~ 50 nights where such conditions preclude the collection of data. Typically, multiple scattering effects are negligible for optical thicknesses less than 0.1, but for thicker clouds ($\tau = 0.2 - 0.6$) the correction can result in a 25 % increase in the optical depth [Reichardt, 1999]. We do not correct for multiple scattering effects for two reasons: first, because this correction would have been, at most, significant for small fraction of the cases involved (categories E and F in Figure 5), and second because the uncertainty (> 100 %) of this adjustment is larger than the correction.

In the calculation of the optical thickness, we assumed a LR of 18.2 sr from Platt and Dille [1984]. This value was determined from lidar measurements (1978 - 1980) in the southern hemisphere. Platt and Dille quote a 20 % error in their LR, but other studies [Ansmann et al., 1993, 1992; Reichardt, 1999], have shown that, depending on the altitude and composition of the cloud, the LR can vary substantially. Therefore, the optical thickness errors are significant ($\sim 10 - 50$ %) with the largest errors found at the cloud base and below [Wandinger, 1998]. A reanalysis of our data using LR's 5 and 50 sr (two extreme values found in the work cited above), leads to SVC frequencies of 40 and 10 %, respectively. Thus it is clear that the value of the LR dominates the error associated with the optical thickness determination. Work done by Ansmann et al. [1993] during the 1989 International Cirrus Experiment (ICE), used

a LR (15 sr) similar to Platt and Dille's when simultaneous Raman measurements were not available to determine LR directly, and justified this choice for optically thin cirrus ($\tau < 0.1$). We choose the value from Platt and Dille, because, the majority of cirrus observed were optically thin and this value has been used by others [Penner et al., 1999].

Another possible source of uncertainty is the temperature measurements. Besides possible systematic errors of the sondes, there is the distance (~ 120 km) between Nîmes and OHP. Two sondes are launched per day from Nîmes, one at noon and another at midnight (universal time). For this work we use the latter sonde, which typically temporally coincided with the lidar measurements. The temperature determinations of the Nîmes' sondes are more accurate than the Raman lidar technique [Hauchecorne et al., 1992]. The tropopause altitude is determined from these measurements using the thermal definition; thus error may be introduced from the definition of the tropopause and from the temperature measurements. For example in Figure 3 there are two consecutive days where the tropopause is greater than 16.8 km, but in both cases there was a second tropopause (~ 10.8 km), which did not meet the WMO definition. Also in Figure 4, 5 % of the cloud top heights were observed at least 1 km above the tropopause, but a more accurate quantification would necessitate temperature sonde launches from OHP.

For the optical thickness measurements, the sondes were used to determine the -25°C threshold. If any part of

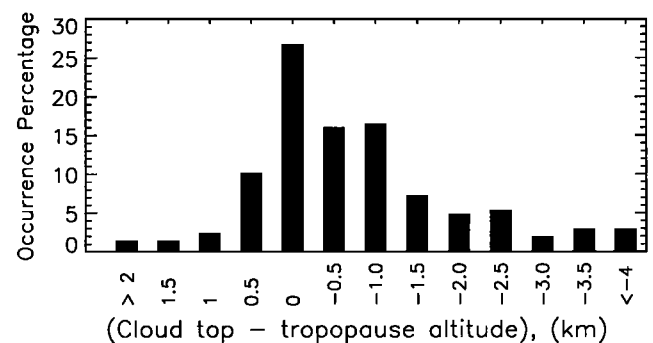


Figure 4. The occurrence distribution of the cloud top heights with respect to the tropopause for 1997 - 1999. Positive values denote cloud top heights above the tropopause.

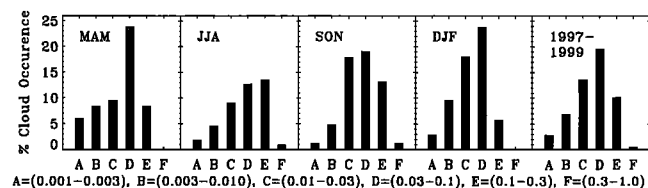


Figure 5. Histograms of cirrus seasonal optical thicknesses binned on a log scale. The first letter of each month is given in the upper left. Lettering along the abscissa corresponds to optical thickness intervals, which are given above. The fifth panel shows the combined results for the three years of data. Categories A - C comprise the SVC component.

the cloud layer was located at or above the corresponding -25°C altitude, then the entire cloud was included in the calculation of the optical thickness. Hence, any errors in the temperature measurements would only slightly affect the optical thickness determinations. Finally, there have been differing ice threshold temperatures quoted for midlatitude cirrus [Heymsfield and Platt, 1984; Roscow et al., 1996; Riedi et al., 1999]. We conducted a reanalysis of our data using a threshold temperature of -40°C . This colder threshold temperature raises the cut-off altitude from ~ 7 km to ~ 9 km. Because most cirrus had cloud top heights above this altitude, this change in threshold had a minimal effect on our results (e.g., an augmentation of only 2% in SVC occurrences).

Conclusions

Our findings of a SVC occurrence frequency of $\sim 20\%$ centered near 10 km confirm the existence of SVC at northern midlatitudes. This is in excellent agreement with the SAGE II zonally average cirrus cloud occurrences at 44°N . While one might expect the lidar to observe fewer cirrus than SAGE II, owing to the different sampling volumes (the SAGE II instrument samples horizontal distances of ~ 200 km), our error analysis shows that there is a possible factor of two uncertainty in the calculated optical thicknesses. This uncertainty is tied to the errors associated with the LR; thus, accurately determining this quantity is essential.

The high altitudinal resolution of our lidar measurements shows that the mean thickness of a SVC is less than 1 km with the distribution skewed towards much thinner layers ($\sim 34\%$ are less than 0.4 km) and that cirrus cloud tops often occur at the tropopause. With nearly 2300 hours of measurements, this is the most extensive lidar study of cirrus available. These results help provide detailed cirrus climatological information that is needed to better model the effect of these clouds on the radiation budget.

Acknowledgments. This work was supported by Snecma and the Université Paris 6 under grant #940480. The authors also gratefully acknowledge the technical support team at OHP and the constructive remarks of the anonymous reviewers.

References

Ansmann, A., J. Bosenberg, G. Brogniez, S. Elouragini, P.H. Flamant, K. Klapheck, H. Linn, L. Menenger, W. Michaelis, M. Riebesell, C. Senff, P.H. Thro, U. Wandinger, and C. Weitkamp, Lidar network observations of cirrus morphological and scattering properties during the International Cirrus

- Experiment 1989: the 18 October 1989 case study and statistical analysis, *J. App. Meteor.*, **32**, 1608-1622, 1993.
- Ansmann, A., U. Wandinger, M. Riebesell, C. Weitkamp, and W. Michaelis, Independent measurement of extinction and backscatter profiles in cirrus clouds by using a combined Raman elastic-backscatter lidar, *App. Opt.*, **31**, 7113-7131, 1992.
- Borrmann, S., S. Solomon, J.E. Dye, and B. Luo, The potential of cirrus clouds for heterogeneous chlorine activation, *Geophys. Res. Lett.*, **23**, 2133-2136, 1996.
- Hauchecorne, A., M.-L. Chanin, P. Keckhut, and D. Nedeljkovic, LIDAR monitoring of the temperature in the middle and lower atmosphere, *App. Phys.*, **B55**, 29-34, 1992.
- Heymsfield, A.J., and C.M.R. Platt, A Parameterization of the particle size spectrum of ice clouds in terms of the ambient temperature and the ice water content, *J. Atmos. Sci.*, **41**, 846-855, 1984.
- Jensen, E.J., W.J. Read, J. Mergenthaler, B.J. Sandor, and L. Pfister, High humidities and subvisible cirrus near the tropical tropopause, *Geophys. Res. Lett.*, **26**, 2347-50, 1999.
- Keckhut, P., A. Hauchecorne, and M.-L. Chanin, A critical review of the database acquired for the long-term Surveillance of the middle atmosphere by the French Rayleigh lidars, *J. Atmos. Ocean.*, **10**, 850-867, 1993.
- Liou, K.-N., Influence of cirrus clouds on weather and climate processes: A global perspective., *Mon. Weather Rev.*, **114**, 1167-1199, 1986.
- Platt, C.M.R., and A.C. Dille, Determination of the cirrus particle single-scattering phase function from lidar and solar radiometric data, *App. Opt.*, **23**, 380-386, 1984.
- Penner, J.E., D.H. Lister, D.J. Griggs, D. J. Dokken, and M. McFarland, *Aviation and the Global Atmosphere: Special Report of the Intergovernmental Panel on Climate Change*, Cambridge University Press, Cambridge, 1999.
- Reichardt, J., Optical and Geometrical Properties of Northern Midlatitude Cirrus Clouds Observed with a UV Raman Lidar, *Phys. Chem. Earth (B)*, **24**, 255-260, 1999.
- Riedi, J., P. Goloub, R. Marchand, and H. Chepfer, Cloud thermodynamic phase from POLDER/ADEOS: Comparison with millimetre wave radar measurements and synoptic weather reports, *In Proceedings of the Europto Conference on Satellite Remote Sensing of Clouds and the Atmosphere IV*, 1999.
- Roscow, W.B., A.W. Walker, D.E. Beuschel, and M.D. Roiter, International Satellite Cloud Climatology Project (ISCCP), Documentation of new cloud datasets, World Climate Research Program (ICSU and WMO), *Tech. Doc. WMO/TD 737*, World Meteorol. Org., Geneva, 1996.
- Rosenfeld, J.E., D.B. Conidine, M.R. Schoeberl, and E.V. Browell, The impact of the subvisible cirrus clouds near the tropical tropopause on stratospheric water vapor, *Geophys. Res. Lett.*, **25**, 1883-1886, 1998.
- Sassen, K., and B.S. Cho, Subvisible-thin cirrus lidar dataset for satellite verification and climatological research, *J. Appl. Meteor.*, **31**, 1275-1285, 1992.
- Sassen, K., M.K. Griffin, and G.C. Dodd, Optical scattering and microphysical properties of subvisible cirrus clouds, and climatic implications, *J. Appl. Meteor.*, **28**, 91-98, 1989.
- Wang, P.-H., P. Minnis, M.P. McCormick, G.S. Kent, and K.M. Skeens, A 6-Year climatology of cloud occurrences frequency from Stratospheric Aerosol and Gas Experiment II observations (1985-1990), *J. Geophys. Res.*, **101**, 29407-29429, 1996.
- Wandinger, U., Multiple-scattering influence on extinction- and backscatter-coefficient measurements with Raman and high-spectral-resolution lidars, *App. Opt.*, **37**, 417-427, 1998.
- Wang, P.-H., P. Minnis, M.P. McCormick, G.S. Kent, G.K. Yue, D.F. Young, and K.M. Skeens, A study of the vertical structure of tropical (20°S - 20°N) optically thin clouds from SAGE II observations, *Atmos. Res.*, **47-48**, 599-614, 1998.

L. Goldfarb, P. Keckhut, M.-L. Chanin, and A. Hauchecorne, CNRS/Service d'Aéronomie, BP 3, 91371 Verrières-le-Buisson Cedex, France. (e-mail: leah.goldfarb@aerov.jussieu.fr)

(Received November 29, 2000; revised January 31, 2001; accepted February 10, 2001.)